ERIKA: Emulating Retarding-field-energy-analyzer Ion Kinetic-transport in Argon-gas

Felipe Soberon[a)]

(Dated: 25 March 2023)

This document reports a one-dimensional simulation of the transport of argon ions across a plasma sheath and through a retarding field energy analyzer (RFEA). The simulation can model DC and AC sheaths. The DC sheath is modeled using Child Law and the AC sheath using the analytical solution of a radio-frequency capacitive sheath by M. A. Lieberman. The model includes elastic and charge exchange ion collisions with background Argon gas.

Keywords: Plasma sheath, Child Law, RF sheath, Charge exchange collision, Retarding Field Energy Analyzer (RFEA)

I. INTRODUCTION

Retarding field analyzers are employed to assess the energy distribution of ions impinging on a surface. Ions acquire considerable kinetic energy as a result of the high voltage across the plasma sheath. This energy distribution is valuable in various applications, such as space propulsion equipment. In other contexts, such as the manufacturing of semiconductor devices, plasma etching equipment, or plasma deposition, the ion energy serves as a parameter that can influence the etch rate, the profile of the process, or the deposition rate.

RFEA devices can be designed as an array of thin grids tightly packed together, with a series of voltages applied to these grids. The primary purpose of this configuration is to select ions based on their energy and to eliminate the detection of electrons originating from the plasma discharge or secondary electrons emitted by the RFEA following ion impact.

The operational range of RFEA devices is limited by several factors, including background gas pressure, fast electrons from the plasma, secondary electrons emitted within the RFEA, ionization occurring inside the RFEA, the distance between RFEA grids, and field distortion within the RFEA caused by space charge.

To assess the impact of any of the factors mentioned above, a computer simulation of a plasma sheath and RFEA grid would enable one to explore these factors individually or in combination.

Here we report a one-dimensional model of a plasma sheath and RFEA device.

II. SIMULATION DESCRIPTION

In this section we provide details of the model. Subsection II.A describe how the space potential and electric field are calculated including the plasma sheath and in the RFEA region. Subsection II.B describe the method to integrate the ion trajectories under the effect of the fields decribed in subsection II.A. Subsection II.C describes the method to simulate ion collisions with the background gas.

II.A. Space Potential and Electric Field

The space potential and electric field are calculated in two regions: the RFEA region, and the plasma sheath. The model is one-dimensional, therefore only space potential and electric field in the z-axis is calculated in these regions. In this geometry, the RFEA is located at $z \leq 0$ and its extension in the negative direction of the z-axis depends on the spaces between the grids and the collector; subsection II.A.1. The plasma sheath starts at $z = 0$ and extends to the plasma, which is located at some $z_{\text{plasma}} > 0$. The location of the plasma sheath boundary edge depends on the plasma sheath model and is further described in subsection II.A.2.

II.A.1. Retarding Field Energy Analyzer

The RFEA modeled includes the standard four grids and collector plate[1]. These are identified as G_0, G_1, G_2, G_3, C. The first grid, G_0, faces the plasma and is at the same potential as the electrode that bounds the plasma discharge. In this model, the voltage of G_0 is set to zero. The second grid, G_1 is typically biased negative respect to G_0 to repel electrons from the plasma discharge. The model does not include electrons, however, this grid is included to simulate the electric field that affects the motion of ions between G_0 and G_1. The third grid, G_2, is used to discriminate ions by setting the voltage of G_2 positive relative to G_0. The voltage of G_2 is typically swept from zero to a large voltage to limit the ion current to the collector and generate the RFEA characteristic voltage-current curve. The fourth grid, G_3, is used to repel secondary electrons that may be emitted by the collector due to ion impact. This grid is usually biased slightly negative relative to the voltage applied to the collector. Again, the model does not include electrons, however, it is included to simulate the electric field between G_3 and the collector that afect the ion trajectories. Finally, the last electrode in the RFEA is the collector, C, which is biased somewhat negative relative to the first grid, G_0.

The model assumes that the grids and non-

dimensional; i.e. zero thickenss. This differs from actual RFEA devices where the grids are usually 40 μm thick (reference some publication by Impedans). Consequently, the model also neglects any lensing effects of non-zero thick grids[2,3]. The distance between grids and the collector are defined in the model as multiples of 100 μm. In actual RFEA devices the grids are physically separated by sheets of Mica, 100μm thick each sheet. The arrangement of grids and spacers is known as the RFEA button stack. For instance, the standard RFEA button stack of a commercial device comprises two spacers between G_0 and G_1, three spacers between G_1 and G_2, three spacers between G_2 and G_3, and two spacers between G_3 and the collector C (reference impedans website Semion). This arrangement is therefore known as a 2332 button stack. The model can simulate the RFEA with any combination of button stack arragements expressed as multiples of the basic spacer.

Besides lensing effects, not included in this model, actual grids are not entirely transparent and a fraction of ions moving through the RFEA are collected by the grids. The transparency of the grids depends on the ion energy and may vary due to the lensing effect. While the model presented here does not simulate these effects it includes a simple transparency factor setting. The user can set this number to any value from 0 to 100%. The transparency setting is common to all grids; i.e., the transparency of grids cannot be set individually.

The space potential between grids is calculated by linear interpolation. Similarly, the electric field between grids is calculated as the potential difference between each grid pair divided by the distance. Figure 1 shows the space potential and electric field in the RFEA for grid voltage settings G_0=0, G_1=-60, G_2=250, G_3=-70, and C=-60 V. The location of the grids and collector is indicated with vertical dashed lines.

II.A.2. Sheath Model

The space potential and electric field in the sheath region of the plasma is determined from the Child Law sheath model for direct-current sheath[4], and from the analytical solution of capacitive radio-frequency sheath for alternate-current sheath[5].

The Child Law sheath size is calculated

$$s_{\text{Child Law}} = \frac{\sqrt{2}}{3}\lambda_D \left(\frac{2V_0}{T_e}\right)^{3/4} \tag{1}$$

Where λ_D is the Debye length

$$\lambda_D = \sqrt{\frac{\epsilon_0 T_e}{e n_s}} \tag{2}$$

Where T_e is the electron temperature (in eV), ϵ_0 is vacuum permittivity (in Farads/metre), e is the basic electric charge (in Coulomb), and n_s is the plasma density at the sheath edge (in m^{-3}).

The voltage in the Child Law sheath is given by

$$V_{\text{Child Law}}(z) = V_0\left(1 - \left(1 - \frac{z}{s_{\text{Child Law}}}\right)^{4/3}\right) \tag{3}$$

Where the position variable, z, is given in metres, and where V_0 is the voltage of the plasma sheath edge relative to the bounding electrode at $z = 0$. The voltage is null at $z = 0$ and V_0 at $z = s_{\text{Child Law}}$. The plasma potential is positive relative to the electrode, therefore V_0 is positive.

The electric field (in V/m) is given by

$$E_{\text{Child Law}}(z) = -\frac{4}{3}\frac{V_0}{s_{\text{Child Law}}}\left(1 - \frac{z}{s_{\text{Child Law}}}\right)^{1/3} \tag{4}$$

Note the field is null at $z = s_{\text{Child Law}}$ and negative otherwise in the sheath region.

Figure 1 shows the space potential and electric field for the DC sheath solution with a voltage across the sheath of 1000 V and plasma density $n_s = 10^{16}$ m^{-3}. Note that even for a small voltage at the discriminator grid G_2 (relative to the plasma potential) the electric fields within the RFEA are much higher than the electic field across the sheath due to the proximity between grids; i.e., ions experience substantially higher forces within the RFEA.

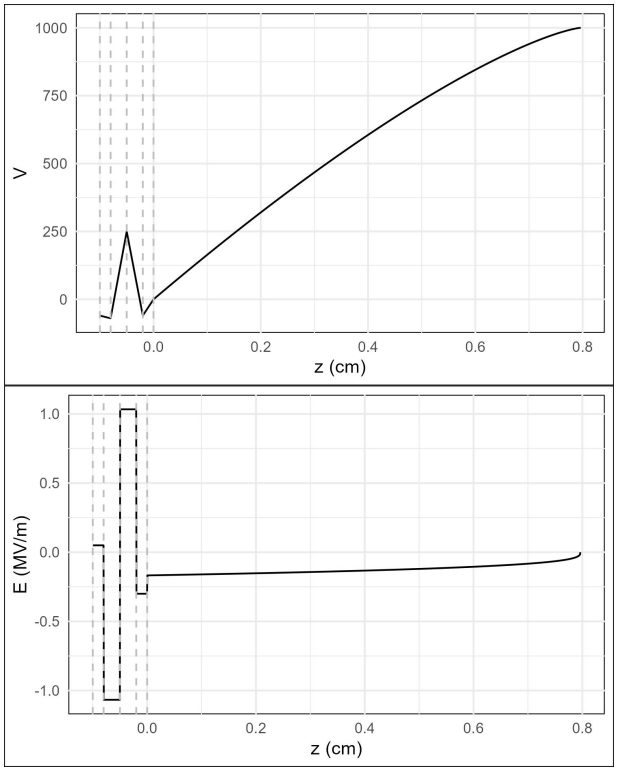

FIG. 1 Space potential across a plasma sheath and RFEA grid stack (top) and corresponding electric field (bottom) for DC plasma sheath with a voltage across the sheath of 1000 V. The edge of the plasma sheath and plasma is at $z = 0.8$ cm. The RFEA is located at $z \leq 0$; with the plasma facing grid (G_0) at $z = 0$. The location of the RFEA grids and collector are indicated by vertical dashed lines.

The space potential and electric field for the AC sheath are calculated using the capacitive sheath solution of reference[5]. The sheath edge of the capacitive radio-frequency discharge changes through the cycle, from col-

lapsing when the voltage across the sheath drops to its minimum to full expansion when the voltage is maximum. The size of the sheath is given by,

$$s(\phi) = s_0(1-\cos(\phi)+\frac{H}{8}\{\frac{3}{2}\sin(\phi)+\frac{11}{18}\sin(3\phi) -3\phi\cos(\phi)-\frac{1}{3}\phi\cos(3\phi)\}) \quad (5)$$

With $\phi = \omega t$ ($\omega = 2\pi f$) and f the radio-frequency. The value of $s(t)$ is limited to ϕ in the range from 0 ($t = 0$) to π ($t = T/2$; where $T = 1/f$ is the radio-frequency cycle period). The size of the sheath at $t = 0$ is zero and its maximum size at $s(t = T/2) = s_m$. The $s(t)$ function can be evaluated at any time value via the following

$$s(t) = \text{abs}(s(\omega\tau(t))) \quad (6)$$

$$\tau(t) = \text{remainder}\left(\frac{t}{T}+\frac{1}{2}\right)-\frac{T}{2} \quad (7)$$

The parameter s_0 is given by

$$s_0 = \frac{J}{en_s\omega} \quad (8)$$

J is the total current through the plasma discharge (mainly displacement current in the sheaths and conduction current in the plasma bulk). The current can be calculated from the plasma density at the sheath edge (n_s) and the maximum voltage across the sheath (V_0)

$$J = \frac{2}{5}\omega\sqrt{\frac{6}{5}}\sqrt{en_s\epsilon_0(\sqrt{576+125V_0}-24)} \quad (9)$$

The H parameter is given by

$$H = \frac{1}{\pi}\frac{s_0^2}{\lambda_D^2} \quad (10)$$

The electric field in the z-direction is given by

$$E_{AC}(z,t) = \frac{J}{\epsilon_0\omega}\{\cos(\omega t)-\cos(\phi(s_m-z))\} \quad (11)$$

If $s(t) < s_m - z$, otherwise the electric field is zero. Note that the function $\phi(s)$ is the inverse of the sheath size $s(\phi)$, that it does not have an analytical solution, and that it is numerically solved in the computer code.

Finally, the space potential for the capacitive radio-frequency sheath is given by the integral

$$V_{AC}(z,t) = \int_0^z E_{AC}(z\prime,t)dz\prime \quad (12)$$

With z in the range from $z = 0$ to $z = s_m$. The field is numerically integrated.

II.B. Ion trajectory integration

II.C. Collisions of ions with background gas

5–8

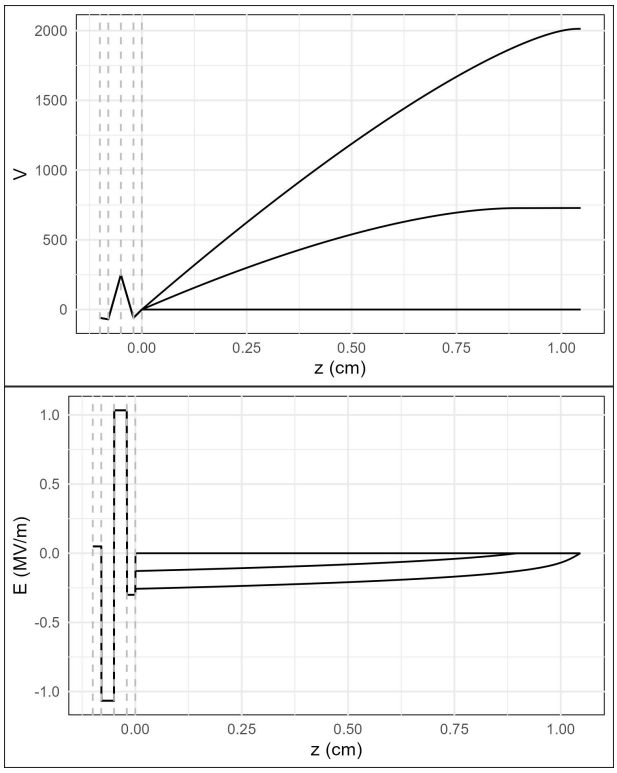

FIG. 2 Space potential across a plasma sheath and RFEA grid stack (top) and corresponding electric field (bottom). The edge of the plasma sheath and plasma is at $z > 1$ cm. The RFEA is located at $z \leq 0$; with the plasma facing grid (G_0) at $z = 0$. The location of the RFEA grids and collector are indicated by vertical dashed lines.

[a] Impedans Ltd.; Electronic mail: felipe.soberon@impedans.com; http://www.impedans.com

[1] I. H. Hutchinson, *Principles of plasma diagnostics* (Cambridge University Press, 1987).
[2] T. H. M. van de Ven, C. A. de Meijere, R. M. van der Horst, M. van Kampen, V. Y. Banine, and J. Beckers, "Analysis of retarding field energy analyzer transmission by simulation of ion trajectories," Review of Scientific Instruments **89**, 043501 (2018).
[3] J. W. Buiter, *Functional analysis of retarding field energy analyzers for ion energy distribution measurements in plasma enhanced atomic layer deposition*, Ph.D. thesis, Eindhoven University of Technology (2018).
[4] M. A. Lieberman and A. J. Lichtenberg, *Principles of plasma discharges and materials processing*, 2nd ed. (Wiley, 2005).
[5] M. A. Lieberman, "Analytical solution for capacitive rf sheath," IEEE Transactions on Plasma Science **16**, 638–644 (1988).
[6] C. Wild and P. Koidl, "Ion and electron dynamics in the sheath of radio-frequency glow discharges," Journal of Applied Physics **69**, 2909–2922 (1991).
[7] B. Bohm and J. Perrin, "Retarding-field analyzer for measurements of ion energy distributions and secondary electron emission coefficients in low-pressure radio frequency discharges," Review of Scientific Instruments **64**, 31–44 (1993).
[8] S. Ries, M. Schroeder, M. Woestefeld, C. Corbella, I. Korolov, P. Awakowicz, and J. Schulze, "Relative calibration of a retarding field energy analyzer sensor array for spactially resolved measurements of the ion flux and ion energy in low temperature plasmas," Review of Scientific Instruments **92**, 103503 (2021).
[9] K. Denieffe, C. M. O. Mahony, P. D. Maguire, D. Gahan, and M. B. Hopkins, "Retarding field energy analyser ion current calibration and transmission," Journal of Physics D: Applied Physics **44**, 075205 (2011).
[10] T. Baloniak, R. Reuter, C. Flotgen, and A. von Keudell, "Calibration of a miniaturized retarding field analyzer for low-termperature plasmas: geometrical transparency and collisional effect," Journal of Physics D: Applied Physics **43**, 055203 (2010).
[11] S. Sharma, D. Gahan, P. Scullin, S. Daniels, and M. B. Hopkins,

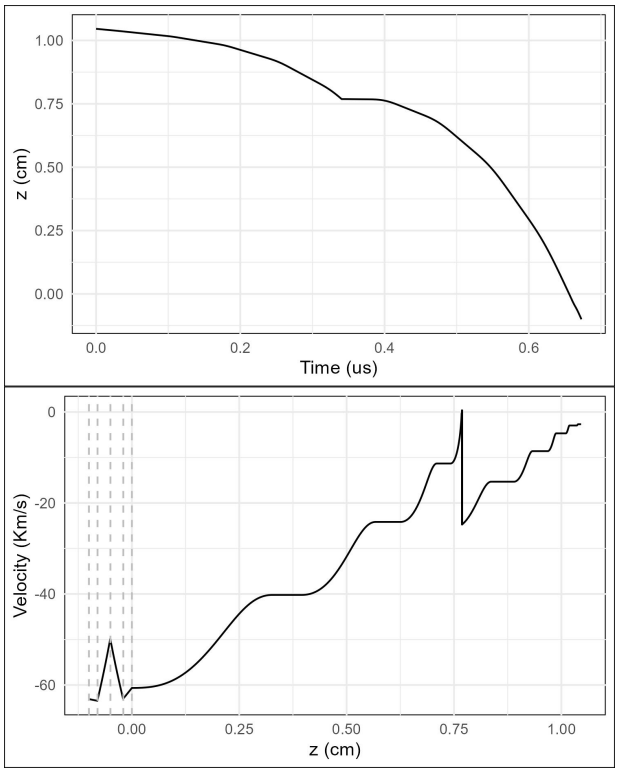

FIG. 3 Sample trajectory of an argon ion from the plasma edge, through the plasma sheath and the RFEA. The edge of the plasma sheath and plasma is at $z > 1$ cm. The RFEA is located at $z \leq 0$; with the plasma facing grid (G_0) at $z = 0$. The location of the RFEA grids and collector are indicated by vertical dashed lines.

"Ion angle distribution measurement with a planar retarding field analyzer," Review of Scientific Instruments **86**, 113501 (2015).

[12]S. Sharma, D. Gahan, S. Kechkar, S. Daniels, and M. B. Hopkins, "A spatially resolved retarding field energy analyzer design suitable for uniformity analysis across the surface of a semiconductor wafer," Review of Scientific Instruments **85**, 043509 (2014).

[13]M. Haass, M. Darnon, G. Cunge, O. Joubert, and D. Gahan, "Silicon etching in a pulsed hbr/o2 plasma. i. ion flux and energy analysis," Journal of Vacuum Science and Technology B **33**, 032202–1 (2015).

[14]W. J. Goedheer, "Lecture notes on radio-frequency discharges, dc potentials, ion and electron energy distributions," Plasma Sources Science and Technology **9**, 507–516 (2000).

[15]L. F. Velasquez-Garcia, J. Izquierdo-Reyes, and H. Kim, "Review of in-space plasma diagnostics for studying the earth's ionosphere," Journal of Physics D: Applied Physics **55**, 263001 (2022).